Materials Science-Poland, 34(4), 2016, pp. 708-714
http://www.materialsscience.pwr.wroc.pl/
DOI: 10.1515/msp-2016-0107

DE GRUYTER OPEN

Enhanced gas-sensing performance of Au-modified ZnO nanoparticles synthesized using bamboo cellulose as a template

YAN LI*, FANG-XIAN ZHAO, XIAO-XUE LIAN

College of Science, Civil Aviation University of China, Tianjin 300300, PR China

Au-modified ZnO (Au/ZnO) nanoparticles (NPs) synthesized using bamboo cellulose template and calcination process were characterized using X-ray diffraction, field-emission scanning electron microscopy, and transmission electron microscopy. The gas-sensing performance of Au/ZnO NPs based sensors was also examined. The results indicated that the Au/ZnO NPs exhibited enhanced gas-sensing performance compared with that of pure ZnO. The response of the Au/ZnO NPs to 100 ppm ethanol (50) at 240 °C was nearly 2.7 times higher than that to acetone (18.4) and approximately 12.5 times higher than that to benzene (4.1), carbon monoxide (1.6), hydrogen (1.6), and methane (1.8), respectively, which demonstrated their higher selectivity to ethanol versus other gases. This high response to ethanol could be attributed to the small size, Schottky barrier, and catalysis.

Keywords: *zinc oxide; gas-sensing; ethanol sensor; Au modification*

1. Introduction

In past decades, with increasing usage of various dangerous gases in many areas, a lot of efforts have been made for development of highly sensitive gas sensors in order to deal with security problems existing in environment, industry and daily life. The crucial works are exploring novel materials with excellent gas-sensing performance to meet these demands. Oxide semiconductor is a suitable material for gas sensor fabrication due to its low cost, physical and chemical stability, easy synthesis, environment-friendliness, high sensitivity and quick response-recovery. In recent years, a large number of preparation methods for highly sensitive oxides with particular morphologies, such as hydrothermal synthesis, sol-gel, thermal evaporation, chemical vapor deposition, flame spray pyrolysis have been developed [1–4]. Gas-sensing properties of various semiconductor oxides, including ZnO, SnO_2, TiO_2, WO_3, CuO, and Al_2O_3, were extensively investigated [5–10] Among these oxides, ZnO – a n-type semiconductor with a wide band gap of about 3.7 eV was considered as a very suitable material for gas-sensing due to its high gas-sensitivity, flexible morphology, lack of toxicity, low cost. It is well known that the properties mainly depend on the morphology, composition, and synthesis approach. Thus, many researches focused on adjusting morphology through various synthesis methods to improve gas-sensing capacity [11–13]. Since gas absorption capacity of sensor materials and the diffusion speed of gas molecules through the gaps between sensing particles are crucial factors for gas-sensing, numerous efforts have been made to prepare mesoporous morphologies with a large specific surface area or to decrease nanoparticle size as far as possible [14–16]. Templates were usually used to fabricate a variety of mesoporous nanostructures of ZnO for sensor applications. Jin et al. [17] reported a bead-like ZnO synthesized using multi-walled carbon nanotubes as template, which showed a very high response to NO_2 gas. Wang et al. [18] synthesized a CuO cage with excellent gas-sensing

*E-mail: liyan01898@163.com

properties using metal-organic frameworks as template. In comparison, biological tissue, with numerous benefits of low cost, abundant availability, hierarchical structure, and environment-friendliness, is considered as an ideal template for fabrication of porous structures. Dong et al. [19] prepared a hierarchical biomorphic ZnO using eggshell membrane as the template. Prakash et al. [20] reported ZnO nanoparticles synthesized using albumen as a biotemplate agent, indicating their good gas-sensing properties. On the other hand, doping other metals into nanostructures is extensively used to improve gas-sensing performance. Li-modified ZnO NPs were reported and the gas-sensing property was investigated, indicating a high response (71.5) to 100 ppm methanol [21, 22]. Au as an excellent dopant has recently attracted much attention for oxide doping. Au particle functionalized ZnO was synthesized and indicated faster response-recovery speed and a higher response to benzene and toluene at 340 °C [23]. Au functionalized porous ZnO was reported and the gas-sensing results revealed that the sensor based on this nanostructure exhibited an enhanced sensing performance towards several volatile organic compounds including n-butanol, ethanol, methanol, acetone and benzene [24]. However, it is still necessary to further develop novel fabrication methods for enhancement of gas-sensing performance in order to meet higher standards in sensor applications in various fields.

In this work, we report an Au-modified ZnO NPs synthesized using bamboo cellulose as a biotemplate. The gas-sensing performance of the sensor based on the as-prepared Au-modified ZnO has been investigated in detail. The sensor shows a high response (50) to 100 ppm ethanol at a relatively low working temperature (240 °C).

2. Experimental

2.1. Materials and apparatus

Zinc acetate ($Zn(CH_3COO)_2$, ⩾99.9 %), acetic acid (CH_4COO, A.R., ⩾98 %), oxydol (H_2O_2, ⩾40 %), auric chloride acid ($HAuCl_4$, Au ⩾47 %), sodium hydroxide (NaOH, ⩾96 %), methanol (CH_4O, 99 %), and ethanol (C_2H_5OH, ⩾99.7 %), all of analytical grade, were commercially purchased and used without any further purification.

Fresh bamboo cellulose pole harvested from the local bamboo forest was firstly decorticated and then cut into small pieces with a length of one centimeter in a vertical rotor cutting mill, discarding the joint parts. The obtained small parts were smashed into cellulose powders with a diameter of 1000 μm, following a drying procedure at 80 °C for 24 h. The powders were treated with a mixture solution of 5 % oxydol (w/w) and 5 % CH_4COO at 80 °C for 2 h. The resulting bleached fibers were treated three times with 2 % NaOH (w/w) solution at 80 °C for 2 h to obtain the pretreated bamboo cellulose (TBC).

Powder X-ray diffraction (XRD) patterns were recorded on a DX-2000 X-ray diffractometer (Dandong Fang-Yuan Instrument Co., Ltd.) operating at 40 kV and 25 mA using a CuKα radiation source ($\lambda = 0.154184$ nm), scanning rate of 0.05°/s for 2θ values of 30° to 65°. The morphology and energy dispersive spectrum (EDS) of the samples was examined using a field-emission scanning electron microscopy (FE-SEM, Hitachi X-650).

The fabrication process of a sensors based on semiconductor oxide has been reported elsewhere [25]. The schematic diagram of a gas sensor has been shown in Fig. 1. A dilute slurry composed of the as-prepared NPs and deionized water was coated onto an alumina tube with a diameter of 1 mm and a length of 6 mm, positioned with a pair of Au electrodes connecting Pt wires. A NiCr alloy coil winded around the tube was employed as a heater to control the operating temperature. Subsequently, the gas sensors were dried in the shade at room temperature for 24 h, then fastened in an aging apparatus at 120 mA for 24 h, following 180 mA for 3 h to get a quick heater-type ZnO gas sensor. The gas-sensing property was measured using a Chemical Gas Sensor-8, intelligent gas-sensing analysis system (Beijing Elite Tech Co., Ltd, China) at a constant room temperature (30 °C) with a humidity (about 25 %). The gas sensitivity was defined as R = Ra/Rg, where Ra and Rg are the sensor resistance in air and in the target

gas, respectively. The time taken by the sensor to achieve 90 % of the total resistance change was defined as the response time for adsorption and the recovery time for desorption. Time spent on diffusion to establish the equilibrium in the measuring chamber is often recorded as a part of the response time, but in fact, it cannot reflect a sensor response to an equilibrium gas. In order to eliminate this problem, we designed a rotatable device that was able to periodically change the sensor exposure to different measuring chambers which were full of equilibrium gas at different concentrations or air (Fig. 2). A gas source with high concentration (5,000 to 20,000 ppm) was achieved by injection of a determined dosage of pure gas (or pure liquid) into a 3 L vessel and kept at 30 °C for 5 h to achieve an equilibrium state. A certain amount of the gas source was extracted using an accurate injector and then respectively injected into different target gas (chambers 2, 4, 6, 8 and 10 shown in Fig. 2) to obtain different concentrations (ppm).

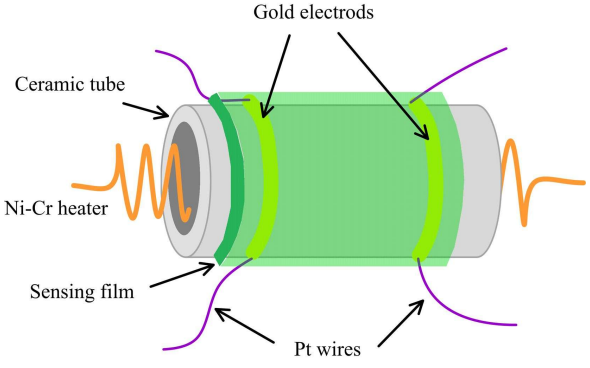

Fig. 1. Schematic diagram of a gas sensor based on the prepared nanoparticles.

2.2. Synthesis of Au/ZnO nanoparticles

A certain amount of TBC was completely soaked in 1 mol/L zinc acetate solution for 3 days. Subsequently the TBC was separated from the solution, then dried at 60 °C and subjected to a calcination process at 700 °C for 5 h to remove bamboo cellulose template in order to obtain ZnO nanoparticles (NPs). The as-synthesized ZnO NPs were added into auric chloride acid solution, meanwhile the pH was adjusted to 7.5 using sodium hydroxide

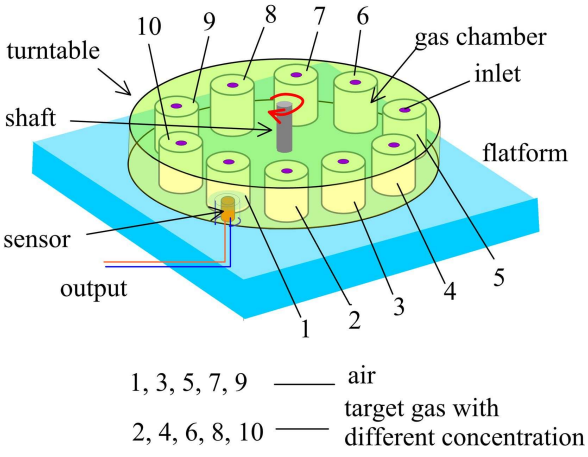

Fig. 2. Schematic diagram of the gas sensor testing measurement system.

solution. A certain amount of methanol was subsequently added into the mixture as a reducing agent. The reaction system was kept at 80 °C under a mild stirring for 3 h to obtain the expected Au/ZnO NPs.

3. Results and discussion

3.1. XRD and FE-SEM analysis

Fig. 3 shows the XRD patterns of the main crystal phases of as-obtained Au/ZnO nanoparticles. For all samples, diffraction peaks corresponding to the (1 0 0), (0 0 2), (1 0 1), (1 0 2), (1 1 0), (1 0 3), and (1 1 2) lattice planes are observed at 31.78°, 34.54°, 36.36°, 47.69°, 56.76°, 62.90°, and 68.13°, respectively, indexed to a hexagonal wurtzite ZnO structure (JCPDS Card No. 36-1451). Au-modification leads to an increase of the FWHM and a decrease of peak intensity, indicating the small crystallite size, which suggests an inhibition effect of Au-modification on the ZnO grains growth. Upon increasing the amount of Au, three characteristic peaks (1 1 1), (2 0 0) and (2 2 0) are clearly observed at 38.17°, 44.39°, and 64.68°, respectively, which correspond to face-centered cubic crystalline Au (JCPDS Card No. 04-0784). This finding indicates that Au exists as a metal crystal phase.

Fig. 4 shows the Au-modification effect on the morphology of the Au/ZnO NPs.

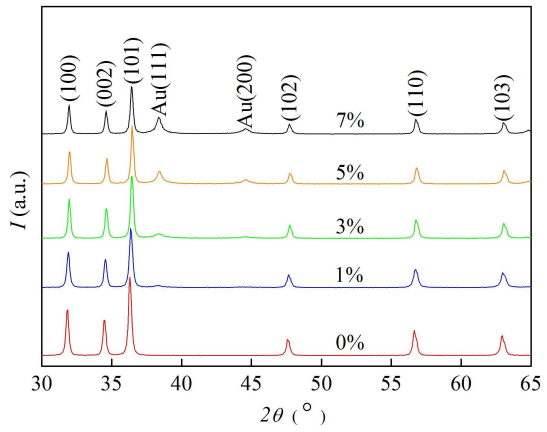

Fig. 3. XRD patterns of Au/ZnO NPs modified with different Au-contents (Au/Zn at.%).

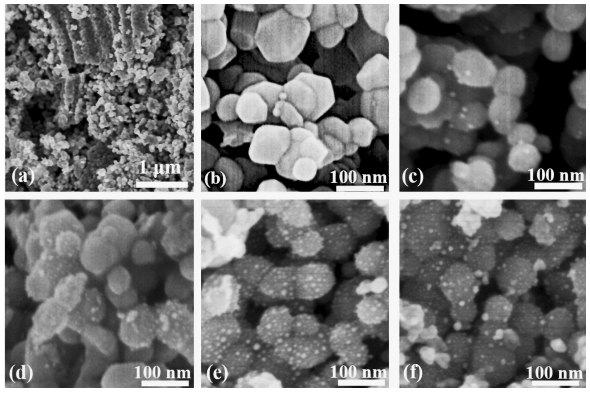

Fig. 4. Overview images of Au-ZnO synthesized using bamboo cellulose template (a) FE-SEM images of Au-ZnO NPs modified with different Au-contents of 0 % (b), 1% (c), 3% (d), 5% (e) and 7% (f).

The overview photograph in Fig. 4a shows a bamboo cellulose-fiber-shaped nanostructure consisting of numerous nanoparticles with uniform diameter. There are a lot of nanopores existing in these nanoparticles, which favors the adsorption, desorption, and diffusion of target gases in the sensing material film, improving its sensing performance. The unmodified ZnO NPs (Fig. 4b) shows a clearly hexagonal morphology with a smooth surface and a grain diameter of 50 nm, indicating a good crystallization state. Au NPs of 5 nm in diameter can be obviously found on the surfaces of all Au-modified ZnO NPs, and the Au NPs density gradually increases with increasing Au content. Meanwhile, Au-modification caused the appearance of nebulous ZnO NPs, which kept the former size unchanged. Au NPs show an extremely good dispersion on the surface of ZnO NPs. In addition, EDS measurement was carried out to confirm Au content in Au/ZnO NPs. Fig. 5 reveals that oxygen, zinc and gold atoms are involved in the obtained Au/ZnO sample, indicating Au nanoparticles actually modified in the prepared ZnO microstructure. The EDS results show that the Au/Zn ratio of the Au(7 at.%)/ZnO is equal to 8 % what is more than that added in the synthesis process. This phenomenon is due to Au NPs located on the surface of ZnO.

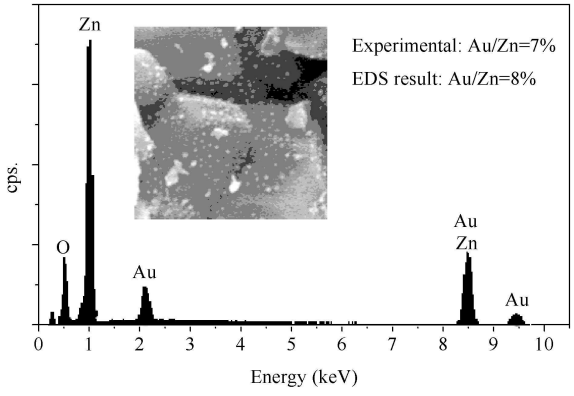

Fig. 5. EDS pattern of the Au(7 at.%)/ZnO NPs.

3.2. Gas-sensing performance

Gas-sensing selectivity is one of the most important properties of gas sensors. Fig. 6 illustrates the gas-sensing response of ZnO and the Au(7 at.%)/ZnO to 100 ppm of different gases including C_2H_6O, C_3H_6O, C_6H_6, CH_4, CO, and H_2. It can be seen that the responses of the Au(7 at.%)/ZnO to the mentioned target gases is higher than that of pure ZnO. The response of the Au(7 at.%)/ZnO based sensor (49.91) to ethanol is 3.2 times higher than that of the pure ZnO. Moreover, the Au(7 at.%)/ZnO based sensor has the highest response to ethanol among all test gases, indicating a higher selectivity to ethanol than to the other gases. It is well known that oxygen species (O^- and O_2^-) are formed on the surface

of a material when ZnO is exposed to air. The oxygen species react with the gases the sensors are exposed to and the resistance of ZnO is changing. For the ZnO material, the chemical-sensing mechanism of ethanol gas is related to its adsorption and/or oxidation of ethanol molecules. The reaction equations are depicted as follows:

$$CH_3CH_2OH_{(gas)} \rightarrow CH_3CH_2O_{(ads.)} + H_{(ads.)} \quad (1)$$

$$H_{(ads.)} + O^-_{(ads.)} \rightarrow H_2O_{(gas)} + e^- \quad (2)$$

During Au catalysis, two steps are involved in the reaction process. First, ethanol can be catalyzed to produce $CH_3CH_2O_{(ads.)}$ and $H_{(ads.)}$, and then $H_{(ads.)}$ reacts with $O^-_{(ads.)}$ to release free electrons back to the conductive band of ZnO NPs. This reaction route makes the reaction between $O^-_{(ads.)}$ and ethanol, as well as adsorption and desorption of oxygen onto the ZnO NPs surface fast.

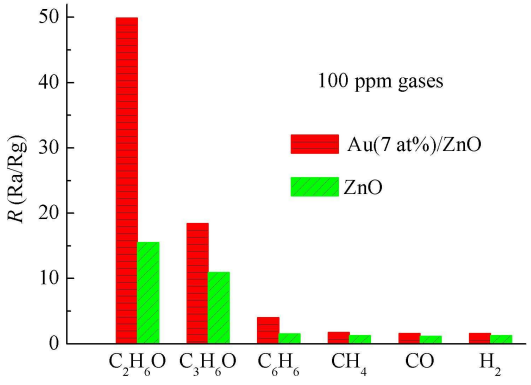

Fig. 6. Responses (R) of ZnO and Au/ZnO NPs to different gases with a concentration of 100 ppm at 240 °C.

Fig. 7 illustrates the responses of Au/ZnO NPs with different Au contents as a function of working temperature from room temperature to 420 °C. It can be seen that the sensing responses of all samples increase and then decrease with operation temperature. It is well known that the gas-sensing process of a semiconductor material involves the adsorption and desorption of gases, and reaction of the adsorbed gases on the surface-active sites of the materials. Sufficient thermal energy across the activation energy barrier is essential for chemisorption and reaction between the gases adsorbed on the surface of the materials. The amount of chemically-adsorbed gas molecules increases with an increase of operating temperature, and the higher sensing response is obtained. However, as the operating temperature further increases, desorption process becomes dominant, resulting in the decrease of the response. The optimum operating temperature at which the response reaches the highest value is ca. 240, 300, and 360 °C for Au/ZnO modified with Au contents of 5 at.%, and 7 at.%, 1 at.% and 3 at.%, and 0 at.%, respectively. We have noted that the response of Au/ZnO NPs increases with increasing Au content. The Au(7 at.%)/ZnO based sensor shows the highest response to 50 ppm ethanol and the lowest working temperature (240 °C) among all samples.

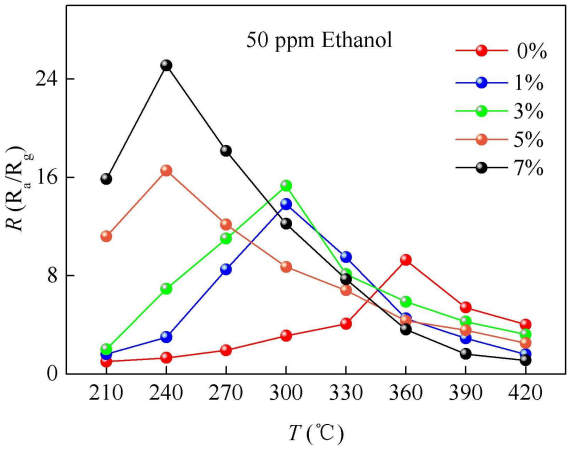

Fig. 7. Responses (R) of Au/ZnO modified with different Au-content versus working temperature (T).

Fig. 8 shows the response of pure ZnO and Au/ZnO NPs as a function of ethanol concentration from 5 ppm to 500 ppm at the operating temperature of 240 °C. The responses of all Au/ZnO based sensors are higher than that of the pure ZnO.

The reliability of semiconductor oxide sensor is another crucial factor to evaluate its gas-sensing performance. The cycle test of the gas-sensing was carried out for the Au/ZnO sensor and the result is shown in Fig. 9. It reveals that the response of

the sensor to 100 ppm ethanol has no decay, indicating high repeatability and aging performance, even if it was exposed to ethanol vapor for several days, which indicates promising detection applications.

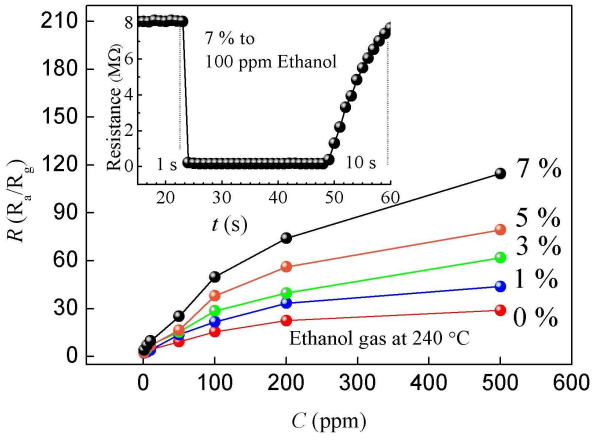

Fig. 8. Responses (R) of Au/ZnO modified with different Au-content versus ethanol concentration (C); the inset shows the resistance related to response and recovery time.

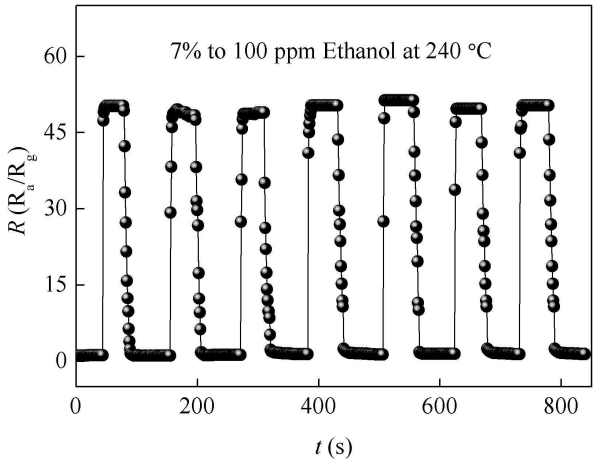

Fig. 9. Gas-sensing cycle test of Au(7 at.%)/ZnO to 100 ppm ethanol at 240 °C.

Herein, Au-modification effects on the response can be explained by Schottky barrier [26] and catalysis [27]. The improvement in the response of the Au/ZnO NPs after Au decoration can be attributed to the electronic and sensitization effects induced by the Au NPs along with the enhancement in resistivity resulting from the formation of heterojunction barrier at the Au/ZnO interface. Since the work function of ZnO (5.2 eV) is slightly higher than that of Au (5.1 eV), the electrons flow from Au to ZnO, establishing a Schottky barrier at the Au/ZnO interface. The electronic sensitization revolves around the formation of electron depletion zones around the metal oxide-noble metal interface and attributes the enhancement in the response to the modulation of the Schottky barrier [1]. Furthermore, the physical/catalytic effects of Au NPs widen the electron depletion in air [28]. Thus, the two aspects actually enhanced the selectivity and response of the sensor to ethanol.

4. Conclusions

In summary, Au-modified ZnO NPs were synthesized using bamboo cellulose fibers as a template. The SEM results revealed that the Au/ZnO NPs have a diameter of ∼50 nm and a hexagonal morphology modified by many Au NPs of several nanometers in diameter. The Au/ZnO NPs based sensor has a fast response and recovery speed, and an excellent reliability for detecting ethanol gas at a relative low working temperature. It seems to be very promising in practical application.

Acknowledgements

This work was financially supported by the Fundamental Research Funds for the Central Universities (No. 3122015L012), Science and Technology Innovation Project 2015 of Aviation Administration of China-study on Air Worthiness Certification Technology of Large Aircraft Cabin Air Environment (No. MHRD20150220), and Large Transport major Projects: Fundamental Research on Large Transport Cabin Air Environment Certification Technology.

References

[1] KANETI Y.V., MORICEAU J.L., LIU M., YUAN Y., ZAKARIA Q., JIANG X.H., YU A.B., *Sensor Actuat B-Chem*, 209 (2015), 889.

[2] ZHAO Q., SHEN Q., YANG F., ZHAO H., LIU B., LIANG Q., WEI A.H., YANG H.Q., LIU S.Z., *Sensor Actuat B-Chem*, 195 (2014), 71.

[3] YU L.Z., SONG H.J., TANG Y.R., ZHANG L.C., LV Y., *Sensor Actuat B-Chem*, 203 (2014), 726.

[4] KRUEFU V., WISITSORAAT A., TUANTRANONT A., PHANICHPHANT S., *Nanoscale Res. Lett.*, 9 (2014), 12.
[5] ZHU D., HU T.X., ZHAO Y.Y., ZANG W. L., XING L.L., XUE X.Y., *Sensor Actuat B-Chem*, 213 (2015), 382.
[6] ZHAO Q.Q., JU D.X., DENG X.L., HUANG J.Z., CAO B.Q., XU X.J., *Sci Rep-Uk*, 5 (2015)
[7] YIN L., CHEN D. L., ZHANG H. W., SHAO G., FAN B.B., ZHANG R., SHAO G.S., *Mater Chem Phys*, 148 (2014), 1099.
[8] YANG Y., TIAN C.G., WANG J.C., SUN L., SHI K.Y., ZHOU W., FU H.G., *Nanoscale*, 6 (2014), 7369.
[9] WU R.J., WU T.M., *Sensor Lett*, 8 (2010), 564.
[10] BURTON P.D., LAVENSON D., JOHNSON M., GORM D., KARIM A.M., CONANT T., DATYE A.K., HERNANDEZ-SANCHEZ B.A., BOYLE T.J., *Top Catal*, 49 (2008), 227.
[11] QURASHI A., YAMAZAKI T., EL-MAGHRABY E.M., KIKUTA T., *Appl Phys Lett*, 95 (2009), 153109.
[12] ZENG Y., ZHANG T., QIAO L., *Mater Lett*, 63 (2009), 843.
[13] GEORGE A., KUMARI P., SOIN N., ROY S.S., MCLAUGHLIN J.A., *Mater Chem Phys*, 123 (2010), 634.
[14] HENLEY S.J., FRYAR J., JAYAWARDENA K.D.G.I., SILVA S.R.P., *Nanotechnology*, 21 (2010)
[15] ZHANG Y., LIU T.M., ZHANG H., ZENG W., PAN F.S., PENG X.H., *J Mater Sci-Mater El*, 26 (2015), 191.
[16] KATOCH A., CHOI S.W., KIM J.H., LEE J.H., LEE J.S., KIM S.S., *Sensor Actuat B-Chem*, 214 (2015), 111.
[17] JIN C., PARK S., KIM C. W., LEE C., CHOI S.W., SHIN K.H., LEE D., *Ceram Int*, 41 (2015), 7729.
[18] WANG Y.T., LU Y.Y., ZHAN W.W., XIE Z.X., KUANG Q., ZHENG L.S., *J Mater Chem A*, 3 (2015), 12796.
[19] DONG Q., SU H.L., XU J.Q., ZHANG D., WANG R.B., *Mater Lett*, 61 (2007), 2714.
[20] PRAKASH T., JAYAPRAKASH R., RAJ D.S., KUMAR S., DONATO N., SPADARO D., NERI G., *Sensor Actuat B-Chem*, 176 (2013), 560.
[21] ZHAO J.W., XIE C.S., YANG L., ZHANG S.P., ZHANG G.Z., CAISTATE Z.M., *Appl Surf Sci*, 330 (2015), 126.
[22] LI Y., LIU M., LV T., WANG Q., ZOU Y.-L., LIAN X.-X., LIU H.-P., *Electron Mater Lett*, 11 (2015), 1085.
[23] WANG L.W., WANG S.R., XU M.J., HU X.J., ZHANG H.X., WANG Y.S., HUANG W.P., *Phys Chem Chem Phys*, 15 (2013), 17179.
[24] WANG L.W., WANG S.R., ZHANG H.X., WANG Y.S., YANG J.D., HUANG W.P., *New J Chem*, 38 (2014), 2530.
[25] FU H.Y., LANG X.Y., HOU C., WEN Z., ZHU Y.F., ZHAO M., LI J.C., ZHENG W.T., LIU Y. B., JIANG Q., *J Mater Chem C*, 2 (2014), 7216.
[26] JU S., KIM S., MOHAMMADI S., JANES D. B., HA Y.G., FACCHETTI A., MARKS T.J., *Appl Phys Lett*, 92 (2008)
[27] LI Y., LV T., ZHAO F.-X., WANG Q., LIAN X.-X., ZOU Y.-L., *Electron Mater Lett*, 11 (2015), 890.
[28] LIN Y.J., DENG P., NIE Y.X., HU Y.F., XING L.L., ZHANG Y., XUE X.Y., *Nanoscale*, 6 (2014), 4604.

Received 2015-10-29
Accepted 2016-09-11